



THE 18th CHESAPEAKE SAILING YACHT SYMPOSIUM

ANNAPOLIS, MARYLAND, MARCH 2007

Corrected Version
with some
additions

Added Resistance in Seaways and its Impact on Yacht Performance

Kai Graf, Institute of Naval Architecture, University of Applied Sciences Kiel (UAS), Germany

Marcus Pelz, R&D-Centre Univ. Applied Sciences Kiel, Yacht Research Unit, Germany

Volker Bertram, Ecole National Supérieur d' Ingeniere, Brest / France

H. Söding, Technical University Hamburg Harburg, Germany

1 ABSTRACT

A method for the prediction of seakeeping behaviour of sailing yachts has been developed. It is based on linear strip theory with some non-linear extensions. The method is capable to take into account heeling and yawing yacht hulls, yacht appendages and sails. The yacht's response amplitude operators (RAO) and added resistance in waves can be predicted for harmonic waves as well as for natural wave spectra. The method is used to study added resistance in seaways for ACC-V5 yachts of varying beam. Results are used for further VPP investigations.

The AVPP velocity prediction program is used to study optimum length to beam ratio of the yachts depending on wind velocity and upwind to downwind weighting. This investigation is carried out for flat water conditions as well as for two typical wave spectra. The results show that taking into account added resistance in seaways has a strong impact on predicted performance of the yacht.

2 NOTATION

$\hat{\sigma}$	Complex amplitude of general harmonic function σ
α	Fin angle of attack
\hat{a}_W	Amplitude of fin angle of attack due to waves
\hat{a}_{S1}	Amplitude of fin angle of attack due to ship motion
\hat{a}_{S2}	Amplitude of fin angle of attack due to ship rotation
$\mathbf{a}_F = \{0, a_{F2}, a_{F3}\}^T$	Vector in fins span wise direction
B	Complex matrix of hydrodynamic masses and damping
c	Average profile length of fin
\mathbf{c}	Sail mean chord vector
c_L	Lift coefficient

c_N	Normal force coefficient
c_M	Added mass coefficient
γ	Peak enhancement factor
D	Water depth
\mathbf{F}_e	Excitation forces due to waves
\hat{F}_{FW}	Added mass force due to waves
\hat{F}_{FS}	Added mass forces due to ship motion
\mathbf{F}_S	Sail lift
ϕ	Potential
$H_{1/3}$	Significant wave height
k	Wave number $k=2\pi/\lambda$
λ	Wave length
λ_l	Significant wave length
Λ	Fin aspect ratio
\hat{L}	Amplitude of fin lift force
M	Yachts mass matrix
m_{ij}	Added mass matrix element
m_F	Fin added mass
m_0	Variance of ship response in natural sea
\mathbf{n}	Normal unity vector
$\mathbf{n}_F = \{0, n_{F2}, n_{F3}\}^T$	Fin normal in y-z-plane
n_{ij}	Damping matrix element
μ	Wave encounter angle
μ_0	Main wave encounter angle
p	Pressure
q	Source strength
r	Reduction factor
R_U	Upright resistance
R_H	Added resistance due to heel
R_I	Induced resistance
R_{PP}	Parasitic profile resistance
R_{AW}	Added resistance due to waves
ρ	Density of water
S	Hydrostatic restoring matrix
s	Fin span
\mathbf{s}	Sail span vector
S_ζ	Sea spectrum

T	Wave period
T_l	Significant period
TWA	True wind angle
$\mathbf{u}=\{u_1, u_2, u_3, u_4, u_5, u_6\}^T$	Vector of ship motion
\mathbf{u}_x	Motion vector of ship sectional strip
\mathbf{u}_S	Motion vector of sail
\mathbf{u}_W	Apparent wind velocity
u_1, u_2, u_3	Surge, sway and heave motion
u_4, u_5, u_6	Roll, pitch and yaw angle
v	Average yacht speed
\hat{v}_{FS}	Amplitude of flow speed normal to fin due to ship motion
\hat{v}_{FW}	Amplitude of flow speed per wave height normal to fin due to wave
W_F	Transformation matrix for fin
W_S	Transformation matrix for sail
ω	Wave frequency $\omega=2\pi/T$
$\omega_e = \omega - \kappa v \cos \mu$	Encounter frequency
$\mathbf{x}_F=\{x_F, y_F, z_F\}^T$	Foils centre of effort
\mathbf{x}_{F1}	Foil reference point
$\mathbf{x}_S=\{x_S, y_S, z_S\}^T$	Sails centre of effort
\mathbf{x}_{S1}	Sails reference point
Y	Response Amplitude Operator RAO
\hat{Y}_{2S}	Transfer Function (TF) for sway at centre of mass
\hat{Y}_{3S}	TF for vertical motion of mass centre
\hat{Y}_5	TF for pitch motion
\hat{Y}_6	TF for yaw motion
\hat{Y}_{zr}	TF for relative vertical motion
dy_w/dx	Inclination of water plane against longitudinal ship axis
$\hat{\zeta}$	Wave amplitude
∇	$\{\partial/\partial x, \partial/\partial y, \partial/\partial z\}^T$

From wave velocity $c_w = \sqrt{\frac{g\lambda}{2\pi}}$ it follows: $\omega^2 = \kappa g$

3 INTRODUCTION

VPPs (velocity prediction programs) allow to predict the performance of sailing yachts for a given set of wind speeds and wind directions. They can thus be used to optimise the main dimensions of a sailing yacht within a given design frame. However accuracy of VPPs depend on proper hydrodynamic modelling of the yacht, in particular accurate prediction of the yacht's resistance. Various methods with reasonable accuracy are available to predict flat water resistance for a yacht canoe body. However prediction of wave resistance of sailing yachts is still error prone. Consequently few VPPs take into account added resistance in seaways, most of them using empirical

methods. This may lead to sub-optimum main dimension ratios if flat water only VPP results are used in the design stage of a sailing yacht.

A design parameter of particular interest in this context is the length to beam ratio of ACC yachts. ACC canoe body beam is a design parameter with no direct impact on the rating of the yacht. It can be chosen freely within given bounds. Since increasing beam usually increases resistance as well as hydrostatic stability, beamier boats are regarded to be strong wind boats while narrow boats are supposed to be better fitted to light wind conditions.

Quantitative measures of this relationship can be derived from VPP studies. This procedure is quite reliable for flat water conditions. However if seakeeping behaviour must be taken into account, accuracy depends on the availability of respective prediction methods capable to take the characteristics of sailing yachts (asymmetric heeled hulls, fins, sails) into account. This was the motivation for the development of a new CFD method for the prediction of seakeeping behaviour and added resistance in waves suitable for sailing yachts.

The method is based on linear strip theory with some non-linear extensions. It is capable to consider heeled ship hulls, appendages, in particular foils and ballast bulbs, and added mass and damping of rolling motion due to sails. It calculates added resistance in harmonic waves as well as in natural wave spectra. The respective program, PDSTRIP, is written in FORTRAN90 and runs on PCs as well as Linux workstations.

By importing PDSTRIP results into our AVPP velocity prediction program the impact of seakeeping behaviour of ACC boats on performance can be studied in detail. The paper sketches the theory behind PDSTRIP and AVPP and the implementation of these methods.

The result of an ACC-V5 yacht beam variation will be shown here. Comparison of flat water VPP results and respective results taking into account natural sea spectra will be given.

4 STRIP METHOD

The strip method is one of the most widely used methods for the prediction of ship motions. It is originated to the work of KORWIN-KROUKOWSKI (1957). PDSTRIP implements the slightly different method of SOEDING (1969). Details of the theory behind PDSTRIP are given by it's author, SOEDING (2006). Here only a very brief sketch of the theory is given.

4.1 Equation of Motion

For harmonic motions $\mathbf{u} = \hat{\mathbf{u}} e^{i\omega t}$ of the vector of the degrees of freedom $\mathbf{u} = \{u_1, u_2, u_3, u_4, u_5, u_6\}^T$ (surge motion u_1 , sway motion u_2 , heave motion u_3 , roll angle u_4 , pitch angle u_5 , yaw angle u_6) the fundamental equation of motions can be derived:

$$(-\omega_e M - B + S)\hat{\mathbf{u}} = \hat{\mathbf{F}}_e \quad (4.1)$$

Here ω_e is the encounter frequency

$$\omega_e = \omega - kv \cos \mu \quad (4.2)$$

(k being the wave number $k=2\pi/\lambda$, ω being the wave frequency $\omega=2\pi/T$, ship speed v and wave direction μ).

M is the real mass matrix of the ship, S is the real matrix due to hydrostatics, B is the complex matrix due to ship motions and $\hat{\mathbf{F}}_e$ are the excitation forces due to the incident wave and its diffraction. In general B is calculated from 2D hydrodynamic forces exerted from the water on a sectional strip moving periodically, see following chapter. The 3-component motion amplitude vector of the strip $\hat{\mathbf{u}}_x = \{\hat{u}_2, \hat{u}_3, \hat{u}_4\}^T$ is related to the respective force vector $\hat{\mathbf{f}}_x = \{\hat{f}_2, \hat{f}_3, \hat{f}_4\}^T$ by:

$$\hat{\mathbf{f}}_x = \begin{bmatrix} \bar{m}_{22} & \bar{m}_{23} & \bar{m}_{24} \\ \bar{m}_{32} & \bar{m}_{33} & \bar{m}_{34} \\ \bar{m}_{42} & \bar{m}_{43} & \bar{m}_{44} \end{bmatrix} \omega_e^2 \hat{\mathbf{u}}_x \quad (4.3)$$

The elements of the complex added mass matrix in (4.3) can be interpreted as real value added masses m_{ij} and damping n_{ij} :

$$\bar{m}_{ij} = m_{ij} + \frac{n_{ij}}{i\omega_e} \quad (4.4)$$

Rewriting (4.3) as time derivative of momentum allows to take into account forward ship speed by introducing substantial derivatives for partial time derivatives ($d/dt = \partial/\partial t - v\partial/\partial x$). Proper transformation of the 3-component strip velocity and forces into the global ship motion coordinate system and integration over ship length allows to calculate B .

A similar approach is used for the excitation forces, the forces acting on the fixed hull generated by an incident wave. These forces consist of the Froude-Krilov part – forces from integration of pressure in the undisturbed wave – and the diffraction part – forces from the diffraction of the wave due to the ship hull. Again 2-D ship section strips are used.

For surge motion a different approach has to be used since strip theory is not capable to predict added mass for surge. Here an empirical formula for the added mass of a strip is used and introduced into the matrix B .

4.2 Calculation of Added Masses, Damping and Excitation Matrices for Sectional Strips

Flow forces acting on sectional strips of the hull are calculated using potential theory. For an oscillating flow in the y - z -plane the potential is expressed as:

$$\phi(y, z, t) = \text{Re}(\hat{\phi}(y, z)e^{i\omega t}) \quad (4.5)$$

The potential of the flow problem is modelled using the patch method, SOEDING (1993). $\hat{\phi}$ is approximated by a superposition of point sources:

$$\hat{\phi}(y, z) = \sum_{i=1}^n q_i \frac{1}{2} \ln((y - y_i)^2 + (z - z_i)^2) \quad (4.6)$$

where q_i is the source strength of the n sources at locations (y_i, z_i) . (4.6) satisfies the Laplace equation (mass conservation for incompressible flow) everywhere except (y_i, z_i) . Therefore point sources are placed within section contour or above water plane.

The following boundary conditions are satisfied (subscripts denote derivatives):

- At the bottom or for deep water:
 $\hat{\phi}_z = 0$ or $\lim_{z \rightarrow \infty} \hat{\phi}_z = 0$
- Linearized free surface condition:
 $\frac{\omega^2}{g} \hat{\phi} + \hat{\phi}_z = 0$
- Along the section contour (normal unity vector on contour \mathbf{n} , complex amplitude of body motion velocity $\hat{\mathbf{v}}$):
 $\nabla \hat{\phi} \cdot \mathbf{n} = \hat{\mathbf{v}} \cdot \mathbf{n}$
- For radiation of waves away from ship hull:
 $\hat{\phi}_y = \mp ik \hat{\phi}$

While panel methods satisfy the above boundary conditions in a collocation point in the middle of each panel, the patch method satisfies the integral of the boundary conditions over each panel (here contour segment). For the boundary condition on the section contour this yields:

$$\int_{\text{Segment}} \nabla \hat{\phi} \cdot \mathbf{n} ds = \int_{\text{Segment}} \hat{\mathbf{v}} \cdot \mathbf{n} ds \quad (4.7)$$

indicating that the average flux over the contour segment must be 0. Slightly more complex expressions arise from the other boundary conditions. Taking into account that any point source contributes to the fluxes of any segment, a linear system of equations evolves, which is solved to calculate q_i .

For known source strengths the potential can be calculated using (4.6) and the pressure from:

$$p = -\rho\phi \quad (4.8)$$

Integration of complex pressure amplitude over strip contour gives flow forces on contour. These flow forces are decomposed into components proportional to ship motion giving radiation forces and forces proportional to wave amplitude giving excitation.

4.3 Foils and Sails

One of the major features of PDSTRIP making it suitable for the investigation of sailing yachts is it's ability to take into account fins like keels and rudders as well as sail.

The algorithm behind PDSTRIP calculates periodic forces perpendicular on fin's centre plane, approximated with the fin's lift. Local flow velocity and angle of incidence of the fin is calculated from the undisturbed incident wave flow field and the motion of the ship. Flow forces are then calculated using linear wing theory. Added masses are calculated from respective coefficients for flat plates. Radiation and diffraction is neglected as well as interaction of multiple fins. For sails a similar approach is used.

4.3.1 Foils

Fins are defined by span s , average chord length c and the centre of effort $\mathbf{x}_F = \{x_F, y_F, z_F\}^T$. Local flow velocity is calculated at an additional point \mathbf{x}_{F1} , normally $c/2$ in $-x$ -direction from \mathbf{x}_F . Orientation of the fin is defined by a unit vector in the y - z -plane normal to fin's centre plane, $\mathbf{n}_F = \{0, n_{F2}, n_{F3}\}^T$.

The amplitude of flow speed in the direction of \mathbf{n}_F generated by the incident wave of complex amplitude $\hat{\zeta}$ and water depth D is:

$$\hat{v}_{FW} \hat{\zeta} = r \frac{\omega \hat{\zeta}}{\sinh(kD)} e^{i(-kx_{F1} \cos \mu + ky_{F1} \sin \mu)} \dots \cdot \mathbf{n}_F \begin{Bmatrix} 0 \\ \sin \mu \cosh(k(z_F - D)) \\ -i \sinh(k(z_F - D)) \end{Bmatrix} \quad (4.9)$$

Here r is a user provided reduction factor taking into account the presence of the canoe body in the vicinity of the fin. From the motion of the ship the complex amplitude of the fin velocity in the direction of \mathbf{n}_F can be derived:

$$\hat{v}_{FS} = i \omega_e W_F \cdot \hat{u} \quad (4.10)$$

with:

$$W_F = \{0, n_{F2}, n_{F3}, -n_{F2}z_F + n_{F3}y_F, -n_{F3}x_{F1}, n_{F2}x_{F1}\} \quad (4.11)$$

The added mass of the fin for \mathbf{n}_F -directed acceleration is:

$$m_F = c_M \frac{\pi}{4} \rho c^2 s \quad (4.12)$$

c_M is a user provided coefficient. For sailing yacht fins of conventional aspect ratio c_M is approximately 1.

The added mass force due to the waves is

$$\hat{F}_{FW} = m_F i \omega r \hat{v}_{FW} \hat{\zeta} \quad (4.13)$$

while the added mass force due to the motion of the ship is

$$\hat{F}_{FS} = m_F \omega_e^2 r W_F \hat{u} \quad (4.14)$$

Beside the added mass forces additional periodic forces are generated due to the time varying angle of attack of the fin $\hat{\alpha}$. The complex amplitude of this force \hat{L} acting in direction \mathbf{n}_F is calculated from the lift of the fin:

$$\hat{L} = \frac{\rho}{2} v^2 s c \frac{dc_L}{d\alpha} \hat{\alpha} \quad (4.15)$$

Here v is average yacht speed and the density is ρ . $dc_L/d\alpha$ is calculated from the effective aspect ratio of the wing $\Lambda = e s/c$, where e is an efficiency factor accounting for details of the fin-canoe body junction. SÖDING (2006) suggests a formula being accurate for small as well as large values of aspect ratio Λ :

$$\frac{dc_L}{d\alpha} = 2\pi \frac{\Lambda(\Lambda + 0.7)}{(\Lambda + 1.7)^2} \quad (4.16)$$

while the formula of TRUCKENBRODT (1969)

$$\frac{dc_L}{d\alpha} = 2\pi \frac{\Lambda}{\Lambda + 2} \quad (4.17)$$

is more widely used for high aspect fins of modern performance yachts. The angle of attack of the fin $\hat{\alpha}$ is calculated from contributions due to the wave:

$$\hat{\alpha}_W = r \frac{\hat{v}_{FW}}{v} \hat{\zeta} \quad (4.18)$$

from contributions of \mathbf{n}_F -directed motion of the ship:

$$\hat{\alpha}_{S1} = -r \frac{\hat{v}_{FS}}{v} = -i\omega_e r \frac{W_F}{v} \hat{u} \quad (4.19)$$

and from contributions due to fin's rotation with the ship:

$$\hat{\alpha}_{S2} = r \{0, 0, 0, a_{F2}, a_{F3}\} \cdot \hat{u} \quad (4.20)$$

where $\mathbf{a}_F = \{0, a_{F2}, a_{F3}\}^T$ is a vector in the span wise direction of the fin, projected on the sectional plane and $|\mathbf{a}_F| = 1$.

Fin forces from (4.13), (4.14) and (4.15) are combined into a single expression. The arising total complex amplitude of the fin forces consists of terms being linearly dependent on ship motion, which contribute to the complex matrix B in (4.1) and of terms being linearly dependent on wave amplitude, which contribute to the excitation forces.

4.3.2 Sail Forces

For the calculation of sail forces a very similar approach has been chosen. A sail or sail set is described by a sail area vector \mathbf{s} normal to the sails planform, where $|\mathbf{s}|$ is the sail area. Additionally the sail sets centre of effort $\mathbf{x}_S = \{x_S, y_S, z_S\}^T$ and the wind velocity reference point $\mathbf{x}_{S1} = \{x_{S1}, y_{S1}, z_{S1}\}^T$. Normally the following relationship holds:

$$\mathbf{x}_{S1} = \mathbf{x}_S + 0.5\mathbf{c} \quad (4.21)$$

where \mathbf{c} is the mean chord vector of the sail. Using this sail definition the force on the sail acting normal to the sail is:

$$\mathbf{F}_S = 0.5\rho_{Air} \mathbf{s} |\mathbf{u}_W - \mathbf{u}_S|^2 c_N \quad (4.22)$$

Here c_N has to be calculated with the sails aspect ratio:

$$c_N = 2\pi \frac{\Lambda(\Lambda + 0.7)}{(\Lambda + 1.7)^2} \alpha \quad (4.23)$$

\mathbf{u}_W is the apparent wind velocity and \mathbf{u}_S the motion of the sail's reference point due to ship motion. For

the complex amplitude of \mathbf{u}_S the following transformation holds:

$$\hat{\mathbf{u}}_S = i\omega_e W_S \hat{u} \quad (4.24)$$

where

$$W_S = \begin{bmatrix} 1 & 0 & 0 & 0 & z_{S1} & -y_{S1} \\ 0 & 1 & 0 & -z_{S1} & 0 & x_{S1} \\ 0 & 0 & 1 & y_{S1} & -x_{S1} & 0 \end{bmatrix} \quad (4.25)$$

Proper linearization of the complex amplitude of the squared velocity difference in (4.22) and the angle of attack yields:

$$\hat{F}_S = -0.5\rho_{Air} |\mathbf{s}| (2\mathbf{u}_W c_N (\bar{\alpha}) + |\mathbf{u}_W| \frac{\partial c_N}{\partial \alpha} \frac{\mathbf{s}}{|\mathbf{s}|}) i\omega_e W_S \hat{u} \quad (4.26)$$

In addition an added mass force is taken into account. It is calculated in a similar way as described for the fins:

$$\hat{F}_{Sa} = -c_M \frac{\pi}{4} \rho_{Air} \mathbf{s} |\mathbf{c}| (i\omega_e)^2 W_S \hat{u} \quad (4.27)$$

The complex sail force amplitudes are transformed into forces and moments acting on the yacht. The combined expression of (4.26) and (4.27), transformed into forces and moments acting on the yacht and reduced by the ships motion vector \hat{u} gives the contribution of the sails to the Matrix B in (4.1).

4.4 Added Resistance due to Waves

Time averaged longitudinal forces \bar{F}_ξ in the inertial coordinate system (moving forward with average ship speed but not following the periodic ship motion) are calculated from three contributions: (i) the periodical force in the ship-fixed vertical direction in combination with the change of that direction, (ii) the force in the ship-fixed transverse direction with the corresponding change and (iii) a contribution from the change of the flows longitudinal momentum due to vertical relative motion of ship and water surface.

$$\bar{F}_\xi = \frac{1}{2} \left(m\omega_e^2 \text{Re}(\hat{Y}_{2s}\hat{Y}_6^* - \hat{Y}_{3s}\hat{Y}_5^*) + 0.5\rho g \sum_{Sib, Port, L} \int \hat{Y}_{\sigma} \hat{Y}_{\sigma}^* \frac{dy_w}{dx} dx \right) \zeta_A^2 \quad (4.28)$$

Here \hat{Y}_{2s} denotes the complex transfer function (TF) for swaying motion of the ship's mass centre, \hat{Y}_{3s}

denotes corresponding TF for heave motion, \hat{Y}_3 and \hat{Y}_6 are TFs of pitch and yaw motion. \hat{Y}_{zr} is the TF for relative vertical motion between ship and water surface at water plane and dy_w/dx is inclination of waterline against the longitudinal ship axis. * denotes the complex conjugate.

4.5 Natural Seaways

For the description of natural seaways a modified formulation of the Jonswap spectrum is used:

$$S_\zeta(\omega, \mu) = H_{1/3}^2 T_1 \frac{177.5 - 6.52\gamma}{(T_1 \omega)^5} e^{-1.25(\omega_M / \omega)^4} \gamma^\Gamma \cdot \left\{ \begin{array}{ll} (\cos^n(\mu - \mu_0)) / f & \text{for } |\mu - \mu_0| \leq \pi/2 \\ 0 & \text{otherwise} \end{array} \right\} \quad (4.29)$$

$$\text{with } \Gamma = e^{-\frac{(\omega - \omega_M)^2}{2\omega_M^2} \left\{ \begin{array}{ll} 0.07 & \text{for } \omega < \omega_M \\ 0.09 & \text{otherwise} \end{array} \right\}^2}$$

Here $H_{1/3}$ is the significant wave height and T_1 is the significant period of the seaway at spectrums centroid. T_1 is linked to a significant wave length λ_1 with:

$$\lambda_1 = \frac{g T_1^2}{2\pi} \quad (4.30)$$

and μ_0 is the main direction of waves. $\omega_M = (4.65 + 0.182\gamma)/T_1$ is the circular frequency of the maximum of the spectrum and γ is a peak enhancement factor. $\gamma=1$ gives the well known Pierson-Moskowitz spectrum while $\gamma=3.3$ gives an average Jonswap spectrum.

$$f = \int_{\mu_0 - \pi/2}^{\mu_0 + \pi/2} \cos^n(\mu - \mu_0) d\mu \quad (4.31)$$

is the integral over the angular spreading function. $H_{1/3}$, T_1 and μ_0 are user provided values, as well as n and γ .

The significant amplitude $r_{1/3}$ of a ship response follows from the variance m_0 , $r_{1/3} = 2m_0^{1/2}$, where the variance m_0 of a ship response is calculated from the spectrum and the RAO:

$$m_0 = \int_0^\infty \int_0^{2\pi} S_\zeta(\omega, \mu) Y^2(\omega, \mu) d\mu d\omega \quad (4.32)$$

The mean added resistance in waves is calculated from the added resistance operator, ARO, the added

resistance for harmonic waves over the wave height squared:

$$RAO(\omega) = R_{AW}(\omega, \zeta) / |\zeta|^2 \quad (4.33)$$

$$\overline{R_{AW}} = \int_0^\infty \int_0^{2\pi} S_\zeta(\omega, \mu) ARO(\omega) d\mu d\omega \quad (4.34)$$

5 AVPP VELOCITY PREDITION PROGRAM

For the prediction of the impact of added resistance in seaways on the performance of the yacht the AVPP velocity prediction program is used. AVPP has been introduced at the 17th Chesapeake Sailing Yacht Symposium 2005, GRAF and BOEHM (2005). Here only the introduction of the term responsible for added resistance in natural seaways is presented.

The total hydrodynamic resistance in the direction of the incoming flow is:

$$R_{Tot} = R_U + R_H + R_I + \sum R_{PP} + R_{AW} \quad (5.1)$$

Here R_{Tot} is total resistance, R_U upright resistance at non-lifting condition, R_H added resistance due to heel, R_I induced resistance due to production of lift and R_{PP} parasitic profile drag of blade and rudder profile. Modelling of these forces is described in detail in the paper mentioned above.

R_{AW} is the added resistance due to natural waves. Generally R_{AW} depends on the geometry of the boat, the wave spectrum, the ratio significant wave length to yacht's waterline length, the main direction of waves μ_0 and the boat speed. PDSTRIP is used to calculate R_{AW} for a range of velocities and main wave directions. This is introduced into AVPP as tabular data:

$$R_{AW} = f(v, \mu_0) \quad (5.2)$$

It is assumed that the main wave direction is linked to the true wind angle TWA:

$$\mu_0 = 180^\circ - TWA \quad (5.3)$$

6 IMPLEMENTATION

PDSTRIP has been implemented in Fortran90. It consists of a single, self contained source file which successfully has been compiled under the Linux and MS Windows operating system. PDSTRIP reads a text file as input, containing a complete description of operation parameters of the yacht with sails and fins and the seaway. In addition an offset table is read.

PDSTRIP is able to process offset files with section contours containing gaps. This way a section of the canoe body and a ballast bulb can be defined. For lower aspect ratios even fins can be described as part of the section contour, however for fins common as yacht appendages they should be defined as described in 4.3.1. using a fin plane normal, a fin centre of efficiency and an effective aspect ratio.

AVPP is implemented using C++, Microsoft Foundation Class for the user interface and OpenGL for 3D graphics. The definition of the hydrodynamic model allows to use input from different sources, may it be towing tank test, CFD calculations or estimation methods from regression formulas. This way AVPP can combine PDSTRIP results for resistance in natural seaways with towing tank test results for the flat water case.

PDSTRIP is available in the public domain and can be downloaded from Sourceforge. AVPP is licensed by YRU-Kiel. Time stamped versions are available as shareware.

7 INTRODUCTION TO THE TEST CASE

The test case for the methods presented here is an investigation of a beam series of ACC yachts measured under the V5 ACC rules. The family is based around a benchmark of beam $B=3.6$ m. Two additional hulls are developed with beam $B=3.0$ m and $B=4.2$ m with constant buoyancy, prismatic coefficient and girth measures. The length of the yachts between girths is $LBG = 20.18$ m. Displacement is $m_M=24$ t for measurement flotation and $m_S=26.65$ t in sailing condition. Fig. 7-1 shows a section line drawing of the benchmark.

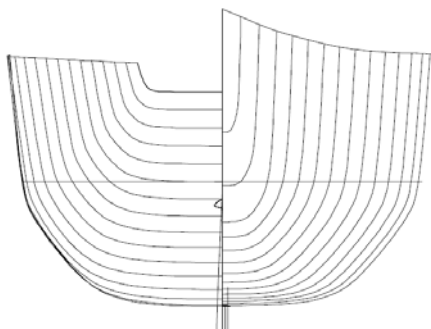


Fig. 7-1: ACC yacht Benchmark at $B=3.6$ m

From the line drawings an offset table has been developed taking into account the canoe body and the ballast bulb, but not the foils. Fig. 7-2 shows a simplified distribution of offset points on canoe body and bulb. For higher accuracy a denser distribution of strips is used for the following computations.

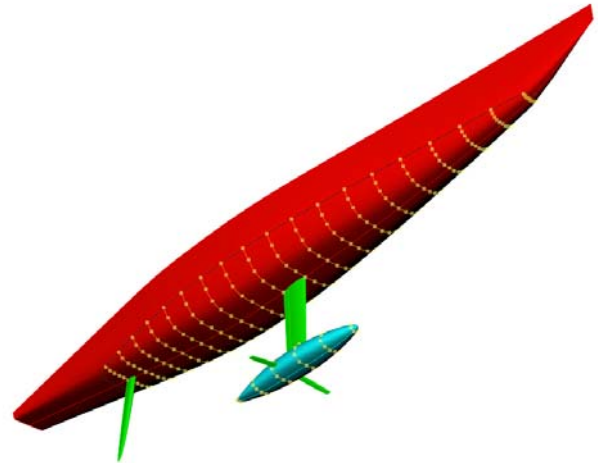


Fig. 7-2: Offset points on canoe body and ballast bulb

As common for strip methods the sectional strip contour ends at the waterline. Increased accuracy can be achieved by using the real dynamic water plane taking into account the generation of waves due to forward speed, however this has been omitted here.

For the benchmark hull towing tank test results have been available for the flat water case. Some of these results have been presented at the last CSYS. These towing tank test results have been used to generate hydrodynamic coefficients for the velocity prediction of the flat water case. For details see GRAF and BOEHM (2005). For the hulls of beam $B=3.0$ m and $B=4.2$ m resistance derivatives with respect to beam:

$$\frac{\partial R_r}{\partial B} = f(v) \quad (7.1)$$

have been calculated from an empirical resistance prediction method for conventional crafts and for Froude numbers up to 0.7, HOLTROP and MENNEN (1982). This way flat water resistance diagrams of the beam variations are calculated, see Fig. 7-3. It is assumed that induced resistance and added resistance due to heel does not change with beam, an inaccuracy accepted within the context of this investigation. This holds also for side force production and centres of efficiency.

In addition to the flat water resistance investigation hydrostatic righting arms are taken into account for the beam variations.

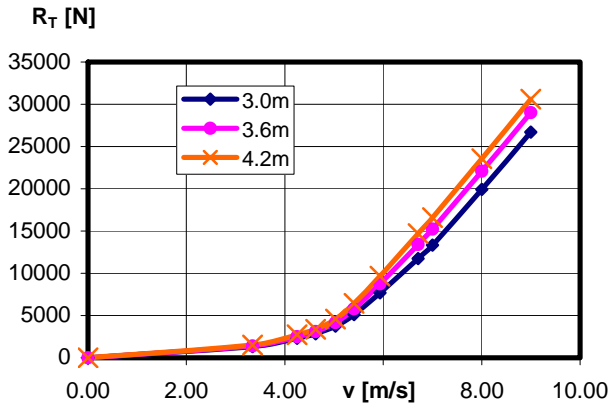


Fig. 7-3: Resistance Diagram for ACC yachts of varying beam

8 FLAT WATER RESULTS OF TEST CASE

The entire study presented here is based around the benchmark AC yacht of beam $B=3.6$ m. For this benchmark the result of a velocity prediction is shown in the velocity polar diagram, Fig. 8-1. The diagram shows the velocity the boat can achieve, depending on true wind angle and wind speed. While accuracy is limited due to restricted towing tank test results available the diagram shows a typical pattern of velocity distribution over the range of wind conditions.

Flat water velocity prediction has been calculated for the benchmark as well as for the yachts with beam variation. For the beam variation the benchmark has been used as a trial horse to calculate time allowance deltas ΔTA . This is the time in seconds the beam variant needs more or less to sail one nautical mile, compared to the benchmark.

Fig. 8-2 shows the time allowance deltas in seconds per nautical mile for the boat of beam $B=4.2$ m. δTA is shown over the range of investigated true wind angles and true wind speeds. Here the calculation is carried out for the upwind sail set only. The diagram shows that the beamier boat shows better performance at low true wind angle for wind speeds of approximately $TWS > 6$ m/s – here indicated by negative values for δTA . For lower wind speed and for higher true wind angles at almost any wind speed the benchmark turns out to be faster. This result has been expected.

Fig. 8-3 shows the same diagram for the narrow boat $B=3.0$ m. A result of similar pattern has been achieved: the narrow boat shows better performance for wind condition where high hydrostatic stability is not needed and the yacht can take advantage from lower resistance.

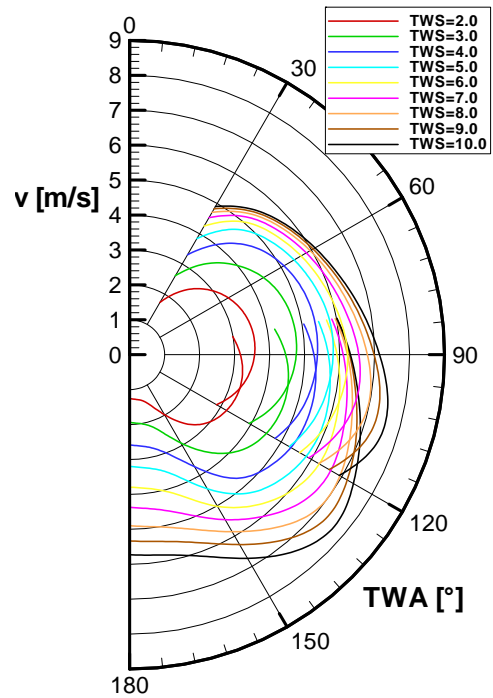


Fig. 8-1: Velocity Polar of Benchmark ($B=3.6$ m)

Time Allowance Deltas for the boat $B=4.2$ m (s/nm)

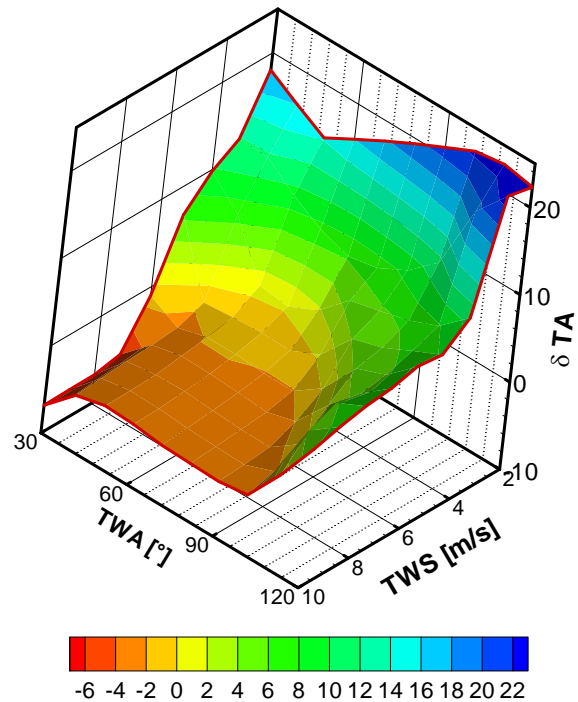


Fig. 8-2: Time Allowance Deltas δTA for the yacht at $B=4.2$ m compared to benchmark (red: beamier boat is faster)

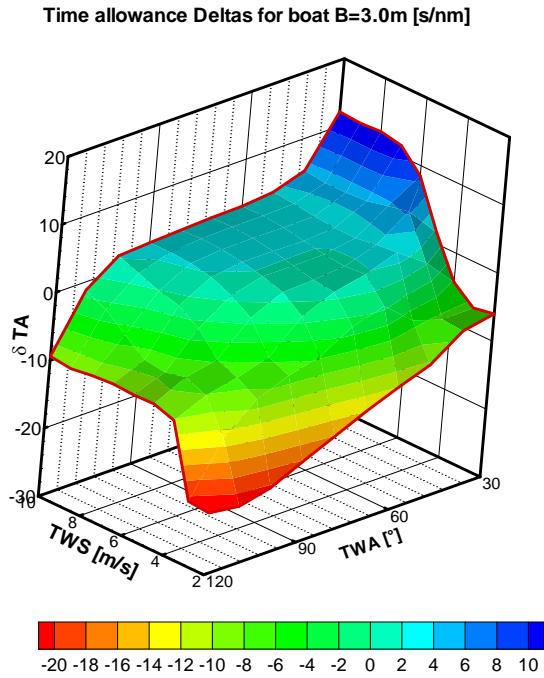


Fig. 8-3: Time Allowance Deltas δTA for the yacht $B=3.0m$ compared to benchmark (red: narrow boat is faster)

Fig. 8-2 and Fig. 8-3 present valuable information for yachts that have to perform on any arbitrary course, for example to compete in distance races. ACC yachts are dedicated to sail Up and Down races, with a focus on the upwind track. Here velocity in windward direction – velocity made good VMG – provides better information. In general this can be derived from diagram Fig. 8-1, giving the expected result: the beamier boat is favoured under strong wind conditions while the narrow boat performs best in light wind. However detailed information about the cross over – the wind velocity where a change in the performance rank occurs – provides valuable information to the designer. Fig. 8-4 shows VMG over true wind speed for the yachts of beam $B=3.0m$, $B=3.6m$ and $B=4.2m$. The diagram shows cross over at $TWS=4.25\text{ m/s}$ for the comparison of the boat $B=3.0\text{ m}$ and the benchmark, and a cross over at $TWS=5.0\text{ m/s}$ for the comparison of the boat $B=4.2m$ and the benchmark. One can also detect that the benchmark shows best general purpose properties: at low wind speed the difference to the narrow boat is small, at high wind speed the difference to the beamy boat is small.

While the accuracy of the cross over prediction is limited due to a lack of towing tank and wind tunnel data, the trend of the results can clearly be detected. It can be obtained that the cross over wind velocities are quite small.

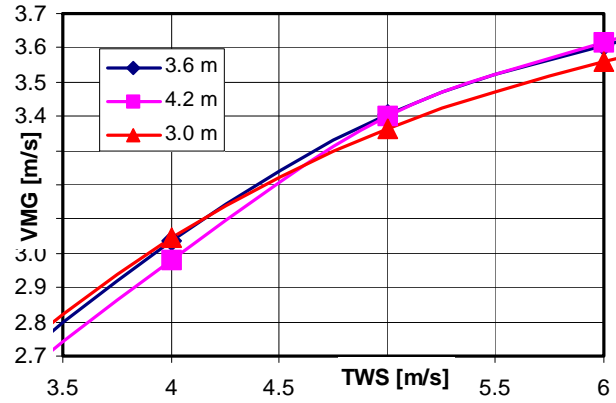


Fig. 8-4: VMG over TWS for an excerpt of investigated wind range

9 ADDED RESISTANCE IN WAVES

Added resistance in waves has been calculated for the benchmark at various boat speeds and a range of main wave directions and for heeling angles of 0° and 27.5° . Fig. 9-1 shows the added resistance in waves R_{AW} of the benchmark at $\varphi=27.5^\circ$ for a Pierson-Moskowitz spectrum, a significant wave height $H_{1/3}=0.42\text{ m}$ and a main wave direction of $\mu=145^\circ$, conforming to a true wind angle of $TWA=35^\circ$ for wind generated seas.

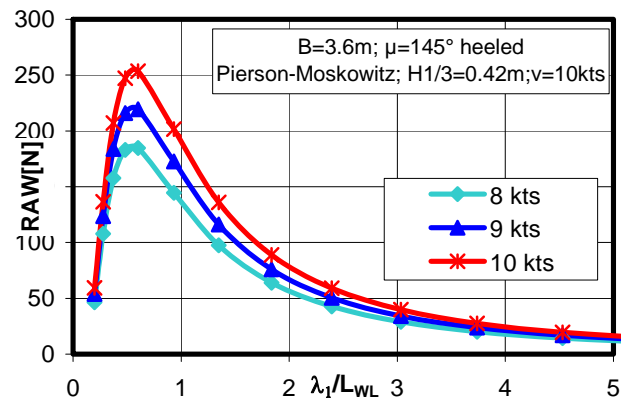


Fig. 9-1: Added Resistance for benchmark $B=3.6m$

For all boat velocities maximum added resistance due to waves occurs at ratios of main wave length to boat's waterline length of approximately 0.5. Here the added resistance reaches approximately 5-7% of the total flat water resistance. It is a well known fact that the strip method gives implausible results for very short waves. However for very short waves it can be assumed that the wave height is relatively small and consequently the added resistance can be assumed to be one order of magnitude lower than the maximum.

Fig. 9-2 shows a comparison of added resistance in waves for different boat beams. Maximum R_{AW} for the boat of

beam $B=3.0\text{m}$ is approximately 60% of the maximum R_{AW} of the benchmark. However the calculation gives no increase of R_{AW} for the boat of beam $B=4.2\text{m}$ compared to the benchmark. While this is not expected it has to be taken into account, that the buoyancy of the boat remained constant for any beam variant. Consequently the boat of beam $B=4.2\text{m}$ has a lower canoe body draft and a pronounced U-shape of its main section. This results in a quite narrow waterline beam for the heeled boat. Maybe this is the reason for the unexpected small difference of added resistance for the boats of beam $B=3.6\text{m}$ and $B=4.2\text{m}$ m.

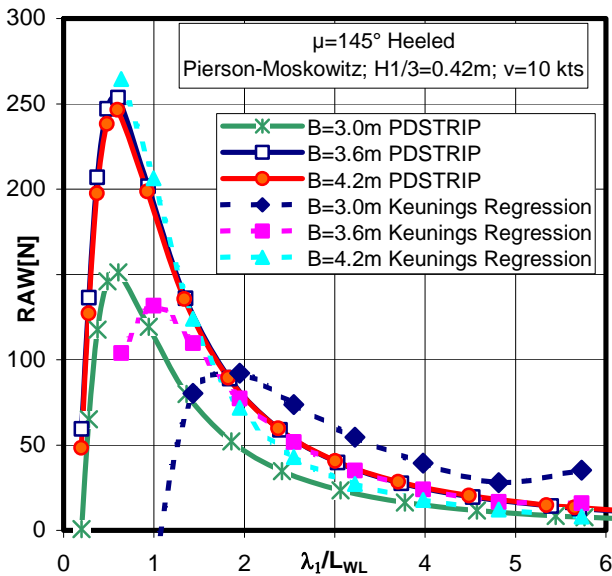


Fig. 9-2: Added Resistance - beam variation

No towing tank tests have been available for the validation of PDSTRIP. However KEUNING and SONNENBERG(1998) provide a regression method to estimate the added resistance in natural seaways. The empirical method of KEUNING and SONNENBERG is based on an analysis of towing tank tests of the Delft Systematical Yacht Hull Series. Two methods for the estimation of added resistance in seaways are provided, however only the so called "7-coefficient-method" is capable to take into account the length to beam ratio.

The method of KEUNING and SONNENBERG calculates the added resistance for the upright yacht only. Appendages are not taken into account. The yacht sails at non-lifting condition.

Comparison of PDSTRIP results with those from KEUNINGs regression show very good agreement for the boat of beam $B=4.2\text{m}$ and wave length to ship length ratios larger than 1. For the yachts of lower beam KEUNING predicts significant lower maximum added resistance, however higher added resistance for long

waves. For low wave lengths and narrow boats the regression results are getting implausible.

It has to be taken into account that KEUNINGS method is based on yacht hulls typical for IMS cruiser racers, yacht of length to beam ratio very different from narrow AC yachts. This may be a reason for inaccuracies for very narrow boats.

Taken into account the restricted comparability of KEUNINGS regression method and PDSTRIP it can be summarized that the achieved accuracy of PDSTRIP is sufficient for variant studies.

10 IMPACT OF BULB, FOILS AND SAILS

The main motivation for the development of PDSTRIP is its ability to take into account foils and sails. The impact of foils and sails is analysed using significant ship motions in natural seaway. Significant ship motions in natural seaways of a Pierson-Moskowitz spectrum are calculated from the response amplitude operator of the respective ship motion, which is calculated in harmonic waves, and from the variance, (4.32).

Fig. 10-1 to Fig. 10-3 show significant heave amplitude, significant pitch amplitude and significant roll amplitude for the benchmark and for different configurations: a) canoe body only, b) canoe body and ballast bulb, c) canoe body, ballast bulb and fins and d) fully appended with sails. Again diagrams show results for a Pierson Moskowitz spectrum, a significant wave height of $H_{1/3}=0.42\text{m}$, a mean wave direction of $\mu=145^\circ$ and the heeled yacht at 10 kts.

Diagrams show that heave amplitude is reduced primary by the fins. For very small and very large wave lengths the impact of foils and sails vanishes.

Also pitch amplitude is reduced significantly by fins. However here sails and the ballast bulb have an impact on pitch amplitude of same order of magnitude. Again for small wave lengths differences between configurations vanish, however for large wave lengths this is not true.

As expected the roll amplitude is affected heavily by fins and sails. For the canoe body roll amplitudes of approx. 8° are generated. Including the ballast bulb roll amplitudes even increase. Maybe excitation due to the bulb prevails damping and hydrodynamic mass forces of bulb. Taking fins into account roll amplitude drops by approx. 2/3. However one has to remember, that excitation due to fins can be of significant order. Sails do not encounter excitation due to waves. Consequently they have a strong reducing impact on roll angle, in particular for higher wind speed.

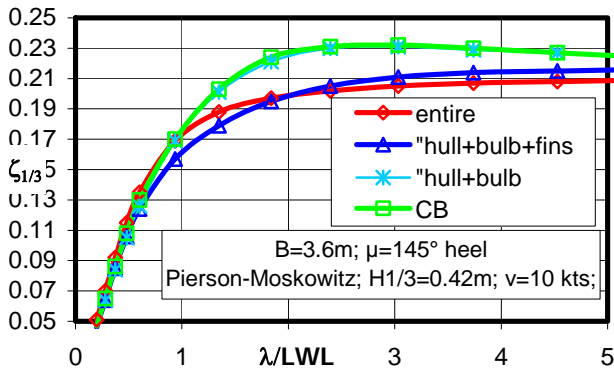


Fig. 10-1: Significant heave amplitude

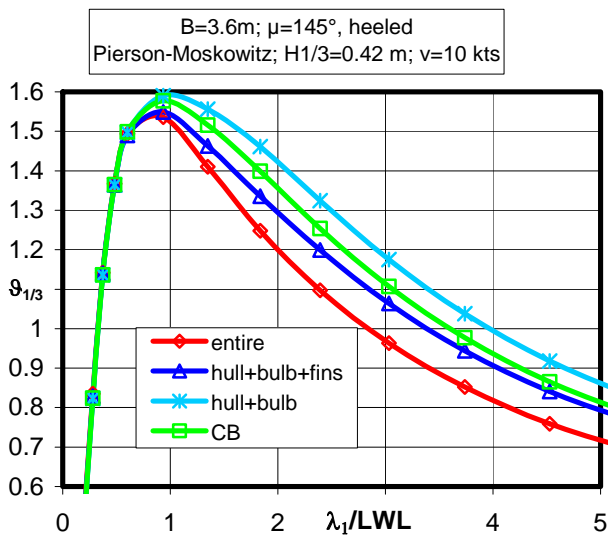


Fig. 10-2: Significant pitch angle amplitude

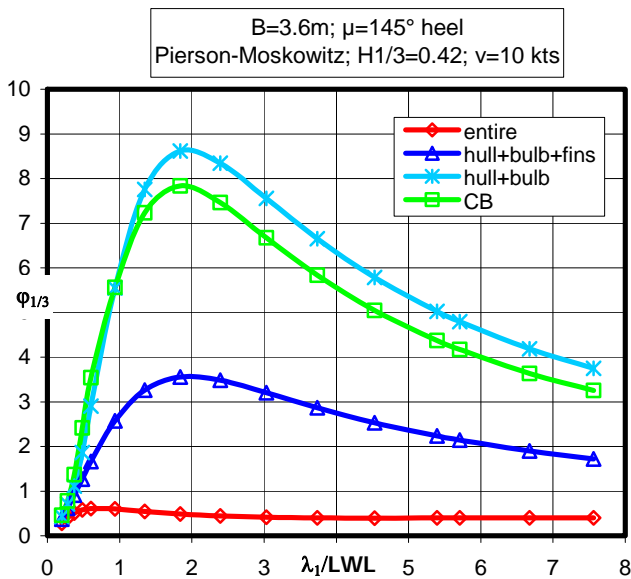


Fig. 10-3: Significant roll angle amplitude

Fig. 10-4 shows a comparison of added resistance in seaways of the four configurations. The diagram shows that the maximum added resistance is affected only marginally by the presence of fins and sails. However for larger wave lengths added resistance due to waves drops by approx. 30% when comparing the canoe body and the fully appended yacht with sails. It is assumed that for smaller wave lengths the first term in (4.28) dominates, where roll motion is not considered, while for larger waves the second term prevails, which includes roll motion indirectly.

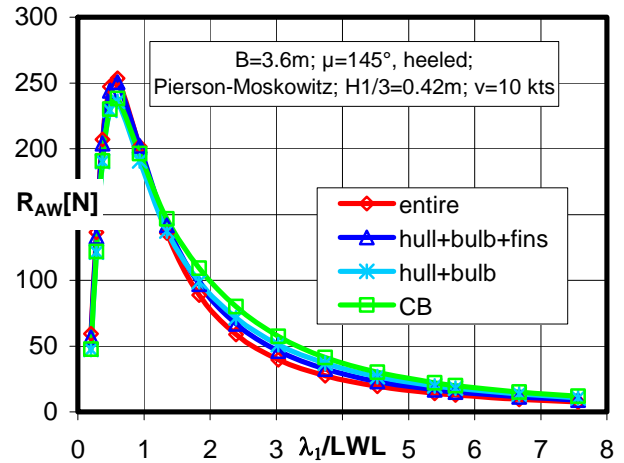


Fig. 10-4: Added Resistance depending on configuration

11 BEAM VARIATION

Added resistance in waves has been integrated into the AVPP velocity prediction program in order to calculate velocity polar diagrams including the impact of sea state on yacht performance.

Added resistance has been calculated for the relevant boat speed range and for ratios of significant wave length to boat length of $\lambda_1/L=0.6$ and $\lambda_1/L=0.9$, see Fig. 11-1. As previously shown added resistance of the yacht $B=4.2$ m resembles benchmark yacht $B=3.6$ m while the narrow yacht $B=3.0$ m shows significantly lower added resistance in natural sea state. This pattern holds for almost the entire boat speed range and for both investigated wave length to ship length ratios.

Based on these added resistance diagram VMG has been calculated for the benchmark and compared with the respective VMG prediction results for the same boat and flat water conditions. Fig. 11-2 shows velocity made good VMG for the benchmark yacht sailing in flat water and in natural seaway, defined by a Pierson-Moskowitz spectrum with significant wave height $H_{1/3}=0.42$ m and a ratio of significant wave length to ship length $\lambda_1/L=0.6$. VMG decreases due to sea state by approximately 0.1-0.08 m/s over the investigated wind speed.

A comparison of VMG of the three beam variants taking into account added resistance unveils that the crossover from the narrow boat to the benchmark as well as the crossover from the benchmark to the beamy boat are at true wind speed of approx. 4.8 m/s. It can be concluded that the benchmark loses its all round properties and the wind speed band width of the narrow boat increases significantly.

There are some restrictions of these results: Significant wave height is assumed not to change with wind speed and results are valid only for the upwind case. Taking into account that wave height usually changes with wind speed would favour the narrow boat even more. For downwind courses narrow boats usually show better performance, taking advantage of the lower resistance where hydrostatic stability is not needed. Taking into account a reasonable weighting of upwind and downwind courses to predict beam cross over should favour the narrow boat even more.

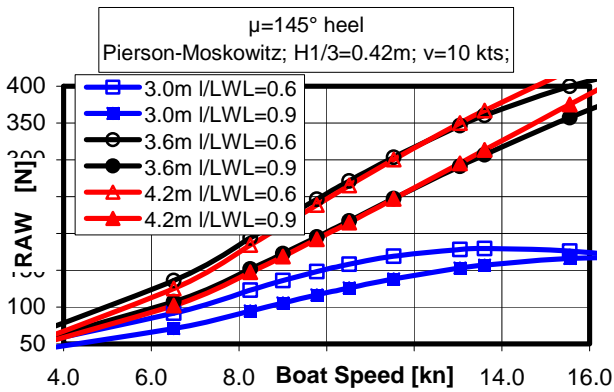


Fig. 11-1: Added resistance depending on boat speed

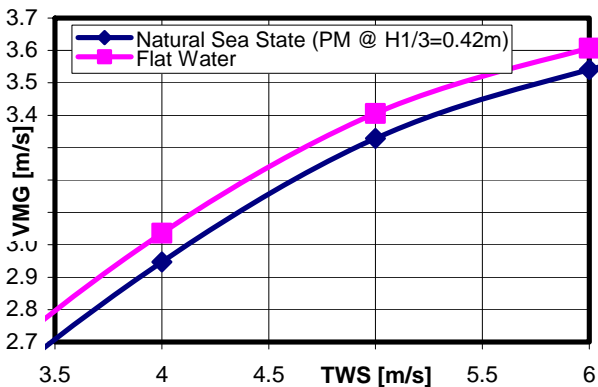


Fig. 11-2: Benchmark B=3.6 m VMG Flat Water and Natural Sea State, $\lambda_1/L_{WL}=0.6$

Wave height is constant for entire range of wind speed. Also for the calculation of wave resistance a heeling angle of 27.5° has been assumed.

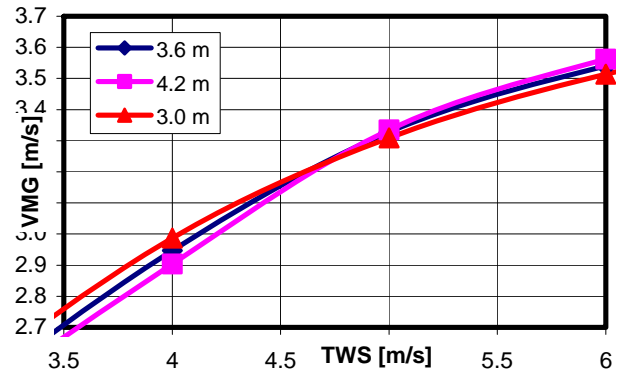


Fig. 11-3: VMG for benchmark and beam variants, RAW taken into account

12 CONCLUSION

PDSTRIP is a new calculation method to predict motion of ships and yachts in natural sea state and added resistance due to waves. PDSTRIP is suitable to be used for sailing yacht investigations since it allows to take into account asymmetric hulls (heeled canoe body of a yacht), ballast bulbs, fins and sails.

PDSTRIP has been used in conjunction with the velocity prediction program AVPP to study impact of added resistance in waves on performance of sailing yachts.

Analysis of ship motion showed that fins and sails do have strong impact on pitch and roll motion, while impact on heave amplitude is small. However maximum added resistance in waves is affected only marginally by fins and bulbs. Only for mean wave length to ship length ratios of 2 to 5 resistance due to the presence of foils and sails drops significantly.

An analysis of the beam series of AC yachts showed strong impact of beam on added resistance for beam smaller than 3.6m. For large beam added resistance does not increase with respect to benchmark, presumably due to narrow flotation beam of the heeled yacht.

Taking into account added resistance due to natural sea state the maximum VMG crossover for beam variation changes, favouring narrow boats at true wind speed, where flat water condition already favours a beamier boat.

While some comparisons of PDSTRIP results with a regression method show reasonable agreement, PDSTRIP currently lacks validation by towing tank test results, favourably with fully appended yachts

13 REFERENCES

- Bertram, V.: Practical Ship Hydrodynamics, Butterworth Heinemann, Oxford, GB, 2002
- Cloughton, A., Wellicome, and Sheno: Sailing Yacht Design / Theory, Addison Wesley Longman Limited, Essex, GB, 1998
- Graf, K. and Böhm, C.: A New Velocity Prediction Method for Post-Processing of Towing Tank Test Results, Proc. 17th Chesapeake Sailing Yacht Symposium, Annapolis, Maryland, March 2005
- Holtrop, J.: A Statistical Re-Analysis of Resistance and Propulsion Data, J. Intl. Shipbuilding Progress, Delft Univ. Press, Delft/NL, 1984
- Keuning, J.A. and Sonnenberg, U.B.: Approximation of the Hydrodynamic Forces on a Sailing Yacht based on the Delft Systematic Yacht Hull Series, 15th Intl. HISWA Symposium on Yacht Design and Yacht Construction, Amsterdam/NL, 1998
- Korwin-Kroukowski, B.V. and Jacobs, W.R.: Pitching and Heaving Motions of a Ship in Regular Waves, SNAME Transactions, 1957
- Söding, H.: Eine Modifikation der Streifenmethode, Schiffstechnik 16, Hamburg, 1969
- Söding, H.: A method for accurate force calculation in flows, Ship Technology Research, Vol. 40, Hamburg, 1993
- Söding, H.: Program PDSTRIP: Public Domain Strip Method, Hamburg, 2006, unpublished
- Truckenbrodt, E. and Schlichting, H.: Aerodynamik des Flugzeuges, Vol. 2, Springer-Verlag, Berlin, 1969